Canadian Mineralogist
Vol. 30, pp. 653-662 (1992)

THE CRYSTAL STRUCTURE OF ALUMOTANTITE: ITS RELATION TO THE STRUCTURES OF SIMPSONITE AND THE (Al,Ga)(Ta,Nb)O_4 COMPOUNDS

T. SCOTT ERCIT[1], FRANK C. HAWTHORNE AND PETR ČERNÝ
Department of Geological Sciences, University of Manitoba, Winnipeg, Manitoba R3T 2N2

ABSTRACT

Two new occurrences of alumotantite, $AlTaO_4$, have been found: the Bikita pegmatite, Zimbabwe and the Alto do Giz pegmatite, Brazil. Alumotantite is biaxial negative with a $2V$ of 66(2)°, η(calc) = 2.21. A new cell with a 4.473(1), b 11.308(4), c 4.775(1) Å, Z = 4, space group *Pbcn* has been assigned, giving a D(calc) of 7.47 g/cm^3. The crystal structure of alumotantite from Brazil has been solved by Patterson and Fourier techniques and refined by a full-matrix least-squares method to an R index of 4.4% for 284 observed (3σ) reflections. Oxygen atoms are nearly hexagonally closest-packed; cations occupy octahedral interstices. TaO_6 octahedra corner-link to form corrugated, perforated sheets normal to Y. Sheets are linked *via* edges to zig-zag chains of edge-sharing AlO_6 octahedra running parallel to Z. A topotaxic relationship between alumotantite and parent simpsonite is observed for samples from Bikita. This reaction involves cation migration through an undisturbed hexagonally closest-packed array of oxygen atoms and is stimulated by an increase in μ_{Ta} of late pegmatitic fluids. A comparison of the structure and inferred field of stability of alumotantite to those of chemically similar ABO_4 compounds suggests that alumotantite is the stable low-temperature polymorph of $AlTaO_4$.

Keywords: alumotantite, crystal structure, mineral data, simpsonite, topotaxy, tantalum oxide, granitic pegmatite, Zimbabwe, Brazil.

SOMMAIRE

Nous avons découvert deux nouveaux exemples d'alumotantite, $AlTaO_4$, dans les pegmatites granitiques de Bikita, au Zimbabwe, et Alto do Giz, au Brésil. Ce minéral est biaxe négatif; l'angle $2V$ est de 66(2)°, et l'indice n calculé est de 2.21. Nous proposons une nouvelle maille: a 4.473(1), b 11.308(4), c 4.775(1) Å, Z = 4, groupe spatial *Pbcn*, ce qui mène à une densité calculée de 7.47. La structure cristalline de l'alumotantite brésilienne a été déchiffrée avec les techniques de Patterson et de Fourier et affinée par moindres carrés avec matrice entière, jusqu'à un résidu R de 4.4% pour 284 réflexions observées (3σ). Les atomes d'oxygène définissent un agencement compact quasiment hexagonal, avec les cations dans les interstices octaédriques. Les octaèdres TaO_6 se joignent à leurs sommets pour définir des feuillets ondulants et perforés perpendiculaires à Y. Les feuillets sont connectés par les arêtes latérales pour former des chaînes en zig-zag d'octaèdres AlO_6 à arêtes partagées parallèles à Z. Une relation topotaxique existe entre alumotantite et simpsonite, son précurseur, dans les échantillons de Bikita. Cette réaction implique une migration des cations à travers un agencement compact hexagonal intact d'atomes d'oxygène, et serait stimulée par une augmentation en μ_{Ta} dans la phase fluide tardive. D'après une comparaison de la structure et du champ de stabilité de l'alumotantite avec ceux de composés ABO_4 semblables, l'alumotantite serait la forme polymorphique de basse température de $AlTaO_4$.

(Traduit par la Rédaction)

Mots-clés: alumotantite, structure cristalline, données minéralogiques, simpsonite, topotaxie, oxyde de tantale, pegmatite granitique, Zimbabwe, Brésil.

INTRODUCTION

Alumotantite, $AlTaO_4$, was first described as a new mineral species by Voloshin *et al.* (1981); it occurs in undesignated granitic pegmatites from the Kola Peninsula. At about this time, during a systematic study of simpsonite, we encountered a mineral resembling alumotantite from the Bikita pegmatite, Zimbabwe. A literature review reveals that this mineral had actually been encountered 35 years earlier by Macgregor (1946). Our electron-microprobe data and X-ray-diffraction studies confirm it as alumotantite. Close inspection of other samples procured for the simpsonite study reveals a third locality for alumotantite, Soledad,

[1]Present address: Research Division, Canadian Museum of Nature, Ottawa, Ontario K1P 6P4.

Brazil. On the basis of geographic, mineralogical and geochemical inferences, we suggest that this sample must have come from the nearby Alto do Giz pegmatite, Rio Grande do Norte, Brazil.

Occurrence and Paragenesis

Alumotantite occurs exclusively in extremely fractionated rare-element-enriched granitic pegmatites. At two of the occurrences, alumotantite is a constituent of albite-rich assemblages of the host pegmatites. At the other occurrence, Alto do Giz, the silicate matrix (to the alumotantite) is completely kaolinized; thus the original assemblage is unknown.

The Bikita occurrence consists of a single albite-rich band 0.3 to 0.5 m thick, underlying a quartz pod in the Mdara mine workings (Macgregor 1946). In our sample, the alumotantite is associated with simpsonite, manganoan tapiolite, manganotantalite, zirconian hafnon, apatite, albite and muscovite. Simpsonite, the most abundant oxide mineral of this association, was the first oxide mineral to crystallize. Alumotantite and the other oxide minerals occur as replacements of, and overgrowths on, the simpsonite.

The Alto do Giz pegmatite undoubtedly represents the best and perhaps also the most abundant occurrence of alumotantite; however, it is also the least understood one from a paragenetic viewpoint. In addition to problems associated with the extensive alteration, the genetic interpretations are further obscured by the fact that at the Alto do Giz pegmatite, Ta minerals were never observed *in situ* by qualified persons (Pough 1945). However, because of the good preservation and intimate association of the oxide minerals, paragenetic relations amongst these minerals can still be inferred. Alumotantite is in direct association with simpsonite, manganotantalite, microlite, parabariomicrolite, and probable lithiowodginite. Simpsonite, manganotantalite, microlite and lithiowodginite mark an earlier generation of oxide minerals; alumotantite and parabariomicrolite appear later and replace certain of these minerals.

The Kola peninsula assemblage has been described elsewhere (Voloshin *et al.* 1981), hence shall only be mentioned briefly here. Alumotantite in the Kola pegmatites is associated with simpsonite, natrotantite, microlite, cesstibtantite and albite. Simpsonite was the first oxide mineral of the association to form; all of the others rim and replace the simpsonite.

Physical and Optical Properties

Alumotantite ranges from colorless (Bikita, Kola) to translucent white (Alto do Giz). Similarly, the luster ranges from adamantine to greasy with increasing opacity. Crystals are subhedral to euhedral, elongate and rectangular to rhombic in cross-section. The crystals are always very small. Alumotantite from Bikita is typically less than 0.1 mm in length, much like the type material (Voloshin *et al.* 1981); that from Alto do Giz is up to 1 mm in length. Crystals of the Bikita material commonly occur as oriented parallel growths on simpsonite, with the axis of elongation of the alumotantite parallel to Z of simpsonite (Macgregor 1946). None of the samples examined shows any cleavage. Because of the small size of the crystals, no determinations of density were possible. The X-ray study, however, gives a calculated density of 7.48 g/cm^3.

In reflected light, alumotantite has higher reflectivity than simpsonite and is also markedly more bireflectant. In transmitted light, it is biaxial negative with a $2V$ of 66(2)° (Alto do Giz sample). None of the indices of refraction of alumotantite is less than 2.00. This is consistent with Gladstone–Dale calculations (mean n = 2.21, constants from Mandarino 1976) and Macgregor's assignment of a birefringence of 0.12.

Chemistry

The samples were analyzed with a MAC 5 electron microprobe operating in the wavelength-dispersion mode. The accelerating potential was chosen as 10 kV for Al$K\alpha$ to minimize absorption [f(χ) = 0.788] and as 20 kV for Ta$L\alpha$ to minimize the atomic number effect; all other lines (Nb$L\alpha$, Sn$L\alpha$) were analyzed at 15 kV. A sample current of 40 nA measured on brass was used. The following standards were used: YAG (Al), cassiterite (Sn), stibiotantalite (Nb) and manganotantalite (Ta). Manganese, iron and titanium also were sought but not detected. Data were reduced by a modified version of EMPADR VII (Rucklidge & Gasparrini 1969) that incorporates the atomic number and absorption correction of Love & Scott (1978) and the characteristic fluorescence correction of Reed (1965).

Table 1 gives all available compositions of alumotantite; for comparative purposes, its ideal composition also is given. Voloshin *et al.* (1981) proposed the formula $AlTaO_4$ for alumotantite; all analyzed specimens conform well to this stoichiometry. Alumotantite may possess minor amounts of Sn (up to 1.0 wt.% SnO_2, Bikita) and Nb (up to 0.8 wt.% Nb_2O_5, Kola) in addition to Ta and Al. Although the data are not sufficiently precise to be conclusive, Sn^{4+} probably substitutes for equal amounts of Al^{3+} and Ta^{5+}, as charge-balance considerations would dictate. Niobium–tantalum isomorphism is very minor to undetec-

TABLE 1. CHEMICAL COMPOSITION OF ALUMOTANTITE

		1	2	3	4
Al_2O_3	wt.%	18.6	18.9	18.5	18.7
SnO_2		0.2	1.0	----	0.0
Nb_2O_5		0.0	0.0	0.6	0.0
Ta_2O_5		81.8	80.9	81.1	81.3
		100.4	100.8	100.4	100.0
		Cations per 16 (O)			
Al		3.96	3.99	3.93	4.00
Sn		0.01	0.07	----	0.00
Nb		0.00	0.00	0.07	0.00
Ta		4.01	3.95	3.98	4.00
		7.98	8.01	7.98	8.00

1. Alto do Giz, Brazil (NMNH 104738); 2. Bikita, Zimbabwe (NMNH 105760); 3. Kola Peninsula, USSR; Voloshin *et al.* (1981); 4. Ideal composition of alumotantite.

"0.0": not detected; "----": not sought

table, most probably owing to a geochemical, not a crystal-chemical control (Ercit 1986).

Structure Analysis

X-ray powder-diffraction patterns of crystal fragments of alumotantite were recorded by the Gandolfi method. The pattern obtained for the sample from Alto do Giz indicated single-phase alumotantite, but patterns for the sample from the Bikita pegmatite persistently showed evidence of contamination by simpsonite. Initially, an attempt was made to index the pattern for the Alto do Giz sample on the cell proposed by Voloshin *et al.* (1981) for the type material, but this failed. In addition, several of the lines reported in the pattern of the type material were not observed in pattern of the Alto do Giz sample, but were found to be present in the pattern of the Bikita sample, suggesting that the type material is contaminated with simpsonite. Examination of the Alto do Giz crystal fragment by the precession method shows that the cell proposed by Voloshin *et al.* (1981) is not truly orthogonal. The diffraction pattern possesses *mmm* symmetry; from the diffraction symmetry, a new set of axes was located, and the diffraction patterns were indexed on this cell. Systematic absences of the types $0kl$ with $k = 2n + 1$, $h0l$ with $l = 2n + 1$ and $hk0$ with $h + k = 2n + 1$ uniquely determined the space group as *Pbcn*. The data for the type material were re-indexed on the new cell, which resulted in cell parameters in good agreement with Brazilian material and standard errors an order of magnitude better than before. The indexed patterns of the Brazilian and type alumotantite are given in Table 2. Cell parameters for all three specimens of alumotantite are given in Table 3.

As a search of the literature showed no compounds isostructural with alumotantite, a structure analysis was undertaken. An equant fragment of dimensions 0.10 × 0.12 × 0.14 mm

TABLE 2. POWDER-DIFFRACTION DATA FOR ALUMOTANTITE

	ALUMOTANTITE NMNH 104738 (Brazil)				TYPE ALUMOTANTITE (USSR)	
hkl	*I* (calc)[1]	*d* (calc)[1]	*I* (obs)[2]	*d* (obs)[2]	*I* (obs)[3]	*d* (obs)[3]
020	17	5.65	30	5.63	50	5.66
110	10	4.16	20	4.16		
021	42	3.65	50	3.64	70	3.64
111	100	3.14	100	3.13	100	3.13
130	47	2.88	60	2.88	80	2.89
040	4	2.83	10	2.82	10	2.83
131	1	2.468				
041	20	2.433	40	2.427	50	2.439
002	11	2.388	30	2.381	30	2.389
200	7	2.237	10	2.234	30	2.238
022	4	2.199	10	2.192	10	2.195
141	4	2.137	10	2.133	20	2.142
102	2	2.106	10	2.102		
220	3	2.080				
112	4	2.071	10	2.072	10	2.068
150	5	2.018	10	2.012	30	2.022
221	14	1.907	30	1.904	40	1.904
060	5	1.885	10	1.881	20	1.884
151	11	1.859	20	1.855	30	1.861
132	24	1.839	40	1.834	50	1.837
042	3	1.824				
240	2	1.754	10	1.752	10	1.754
241	21	1.646	40	1.644	50	1.649
202	12	1.632	30	1.629	40	1.633
222	2	1.568	10	1.566	10	1.563
152	4	1.541	10	1.539	20	1.543
023	3	1.532	10	1.526	20	1.528
170	2	1.519	10	1.516		
113	8	1.487				
062	4	1.479	20	1.475	30	1.483
310	1	1.478				
171	8	1.448	30	1.444	30	1.448
260	3	1.441				
242	2	1.414				
080	2	1.414				
311	6	1.412	20	1.410	40	1.413
043	7	1.387	20	1.382	40	1.388
330	5	1.386				
081	3	1.355	10	1.352	20	1.357
172	2	1.282	10	1.278	10	1.281
223	3	1.264	10	1.262	20	1.264
153	2	1.250	10	1.246	10	1.249
350	1	1.245				
262	4	1.234	10	1.231	30	1.235
082	1	1.216				
190	2	1.210	10	1.207	10	1.212
351	2	1.205				
332	5	1.199	10	1.197	20	1.200

1. Calculated (from the refined structure with the program DBW 2.9, Wiles & Young 1981) for a powder diffractometer equipped with an automatic divergence slit. Only reflections with $I > 1$ are reported.
2. 114.6 mm Gandolfi camera; Ni-filtered Cu radiation. Corrected for shrinkage but not absorption.
3. Voloshin *et al.* (1981). 114.6 mm powder camera, unfiltered Fe radiation.

TABLE 3. UNIT-CELL PARAMETERS (Å) FOR ALUMOTANTITE

	1	2	3
a	4.473(1)	4.46	4.477(1)
b	11.308(4)	11.29	11.309(3)
c	4.775(1)	4.76	4.767(1)

1. Alto do Giz, Brazil (NMNH 104738). Four-circle diffractometer, MoKα radiation, graphite monochromator.
2. Bikita, Zimbabwe (NMNH 105760). Precession camera, Zr-filtered MoKα radiation.
3. Kola Peninsula, USSR. Refined from the data of Voloshin *et al.* (1981).

was used for the collection of intensity data. Data were collected with a Syntex $P2_1$ automatic four-circle diffractometer over one asymmetric unit, to a maximum 2θ of 60° using Mo$K\alpha$ radiation. A total of 446 reflections were measured, of which 284 were considered observed (greater than 3σ). Of these, four very weak reflections (only slightly greater that 3σ) violating *Pbcn* group symmetry were removed from the set. The highly absorbing characteristic of the material (μ = 480 cm^{-1}) necessitates an absorption correction; both spherical and ψ-scan corrections were applied to the data. Cell dimensions were obtained from the least-squares refinement of a subset of reflections

TABLE 4. CRYSTAL DATA FOR ALUMOTANTITE

a: 4.473(1) Å	Crystal size:	1.7 x 10^{-3} mm³
b: 11.308(4)	μ (Mo$K\alpha$):	480 cm^{-1}
c: 4.775(1)	Total no. of $\|F_O\|$:	446
Space group: *Pbcn*	No. of $\|F_O\| > 3\sigma$:	284
Z: 4	Final R (obs):	4.4%
D (calc): 7.48 g/cm³	Final R_w (obs):	5.5%

Temperature factor form used: $\exp(-\Sigma\Sigma h_i h_j \beta_{ij})$

$R = \Sigma(|F_O|-|F_C|)/\Sigma|F_O|$

$wR = [\Sigma w(|F_O|-|F_C|)^2/\Sigma w|F_O|^2]^{1/2}$, $w = 1$

automatically aligned on the diffractometer. Miscellaneous information about the refinement is given in Table 4.

Consideration of the proposed stoichiometry and of possible densities for alumotantite indicates that the true cell of alumotantite contains four formula units. Assuming complete order among cations, Al and Ta were assigned to separate 4*c* sites (Wyckoff notation). While the diffractometer intensity data were being collected, an *hk*0 Patterson projection was made from precession camera intensities; Ta–Ta vectors were located, giving $y_{Ta} = 0.17$.

The program RFINE of Finger (1969) was used for the structure refinement. Scattering curves for neutral atoms were taken from Cromer & Mann (1968) and anomalous scattering factors were from Cromer & Liberman (1970). The composition of the sample used in the refinement was approximated as $AlTaO_4$. In the first stage of the solution, the position of the Ta atom was refined. A difference Fourier map was then constructed, from which the Al position was located. The cation positions were refined, and a ΔTa,Al map was constructed. The map suggested that oxygen atoms occupy four 8*d* sites, not the two expected from the stoichiometry. Nevertheless, the positions of all four sites were entered in the refinement. The isotropic temperature-factors of the oxygen atoms clearly indicated that two of the four were false, with mean $B = 4.5$ Å^2; these two were discarded from the refinement. Two more cycles of refinement with isotropic temperature-factors reduced the conventional *R* index from 13.9% to 5.0%. A difference Fourier map at this stage showed no unexpected anomalies. The tantalum and oxygen atoms were modeled as vibrating anisotropically (aluminum could not be realistically refined anisotropically), and a secondary extinction correction was applied, resulting in a final *R* index of 4.4%.

Bond-valence calculations [using the constants of Brown (1981) and Ercit (1986)] showed that the sums to the cations differ from their ideal values: Σs(Ta) = 4.7 *v.u.*, Σs(Al) = 3.2 *v.u.*, possibly owing to cation disorder. An attempt was made to refine the degree of order in the cationic sites according to the constraint: nunber of Al atoms = number of Ta atoms = 4 per unit cell, which is in agreement with results of microprobe analyses (Table 1). The model converged on a fully ordered scheme (0 Al atoms in the Ta site and *vice versa*), which indicates that cation disorder is not the cause for the deviation in bond-valence sums. To assess whether an error in the absorption correction could be responsible for the bond-valence deviations, the experiment was repeated. Collection of the second data-set followed the same procedure as for the first, except that data were collected with a Nicolet *R*3*m* diffractometer according to the experimental method of Ercit *et al.* (1986). Although the second refinement converged at a marginally improved conventional *R* of 3.9%, the resulting positional parameters are not significantly different from those of the first refinement. From this agreement, we conclude that potential errors in the absorption correction do not significantly affect the positional parameters, and thus are not responsible for the slight deviation in bond valence.

Observed and calculated structure-factors for both refinements are available from the Depository of Unpublished Data, CISTI, Natural Research Council of Canada, Ottawa, Ontario K1A 0S2. Because of the similarity of the two refinements, we present atomic positional and thermal parameters for the first refinement only in Table 5.

TABLE 5. POSITIONAL AND THERMAL PARAMETERS FOR ALUMOTANTITE

Atom	*x*	*y*	*z*	*B* (Å²)
Ta	0	0.16817(9)	1/4	0.41(3)
Al	0	0.4346(7)	1/4	0.44(11)
O1	0.222(4)	0.312(1)	0.086(4)	0.54(23)
O2	0.266(4)	0.058(1)	0.073(4)	0.66(25)

Atom	β_{11}	β_{22}	β_{33}	β_{12}	β_{13}	β_{23}
Ta	62(5)	4(1)	55(5)	0	-2(8)	0
O1	45(66)	13(9)	63(57)	-9(23)	-3(62)	-2(24)
O2	132(72)	2(8)	90(66)	0(22)	-98(77)	0(21)

All β_{ij} are Å² x 10^4

DESCRIPTION OF THE STRUCTURE

The array of oxygen atoms of the alumotantite structure is approximately hexagonally close-packed (Fig. 1). The close-packed layering is perpendicular to *X*. Cations occupy half of the octahedral interstices of the oxygen array. Considered in terms of polyhedra, each level perpendicular to *X* consists of branched, zig-zag chains of edge-sharing, slightly distorted octahedra running parallel to *Z*. AlO_6 octahedra make up the backbone of these chains; TaO_6 octahedra are attached laterally to this backbone. The gross configuration of the chains is the same for all levels.

A projection along *Y* (Fig. 2) illustrates the

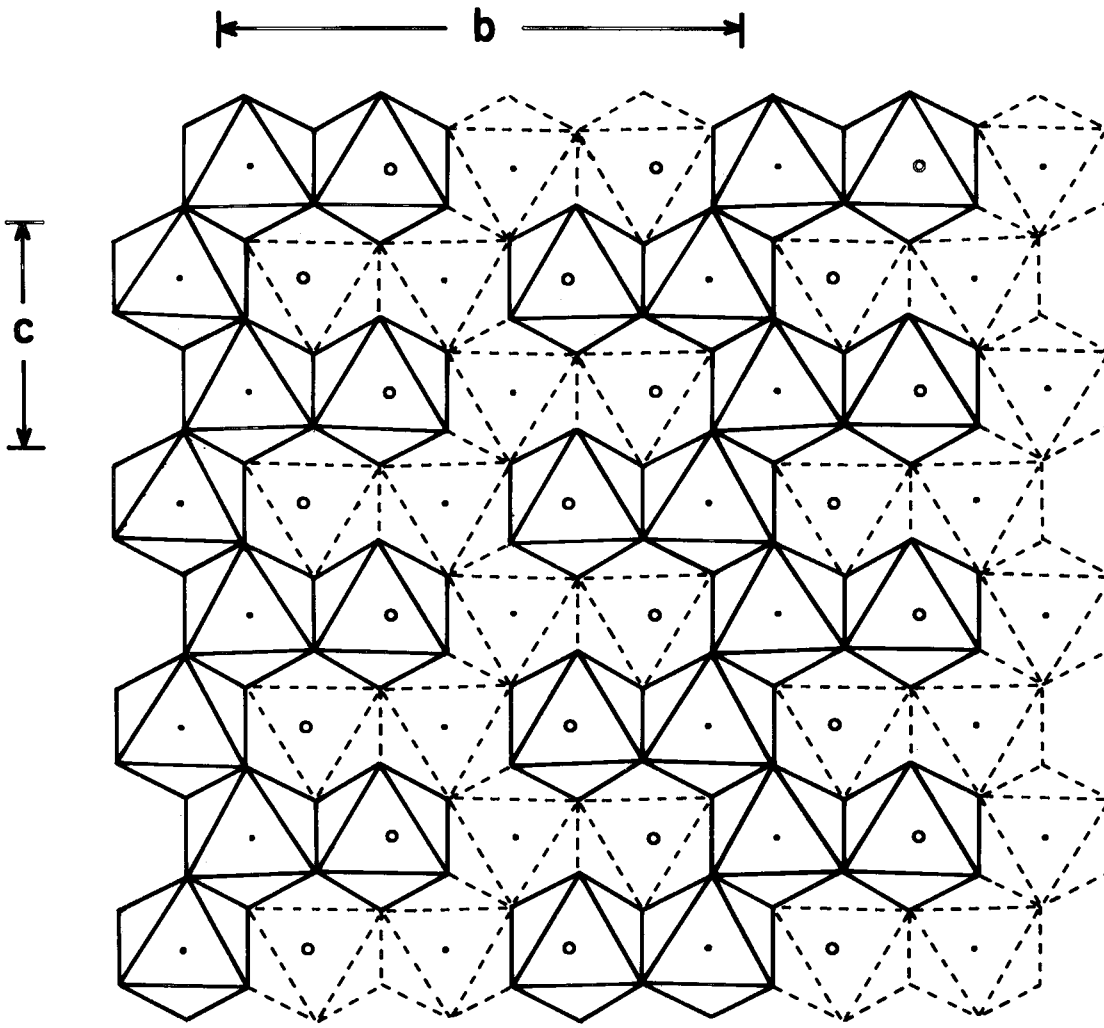

FIG. 1. Projection of the alumotantite structure along *X*. Occupied octahedra of one layer are in solid lines, those of the next layer down, in broken lines. Each occupied octahedron is immediately overlain and underlain by an unoccupied one. Aluminum atoms are denoted by filled circles, tantalum atoms, by open circles. The unit cell is two layers deep.

interrelationship of the TaO_6 polyhedra. Each octahedron shares four corners with two octahedra above and two below it. The result is a perforated, corrugated sheet of tantalum-bearing polyhedra normal to *Y*. Each sheet is linked to neighboring sheets by edge-sharing with the backbone of aluminum-bearing polyhedra.

Interatomic distances and angles are presented in Table 6. Details of the two types of polyhedron in alumotantite are given in Figure 3. The Ta–O and Al–O distances compare very well with calculated values from Shannon (1976) ($Ta–O_{obs}$ = 2.008, $Ta–O_{calc}$ = 2.00; $Al–O_{obs}$ = 1.893, $Al–O_{calc}$ = 1.895 Å), supporting the earlier conclusion of full order between cations. Deviations of the coordination polyhedra from ideal octahedral geometry are slight. Most deviations can be rationalized in terms of cation–cation repulsions and number and location of shared edges. The aluminum-bearing octahedron possesses three shared edges regularly disposed about the polyhedron. Two of these edges are shared with adjacent aluminum-bearing octahedra and one with an adjacent tantalum-bearing octahedron. Because

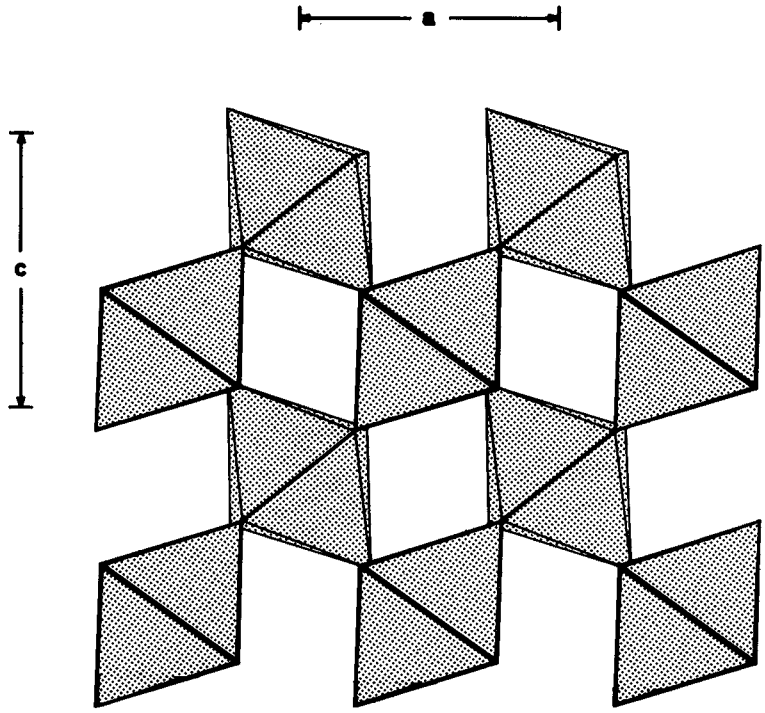

FIG. 2. Projection of the sheet of tantalum–oxygen polyhedra down *Y*.

of this immediate environment of nearly-balanced repulsions, the aluminum atom lies near the geometric center of its coordination polyhedron. Because the tantalum–oxygen octahedron shares only one edge and because the Ta–Al interatomic vector lies along *Y* (the only positional variable for the tantalum atom), tantalum–aluminum repulsion distorts the tantalum octahedron more than the aluminum octahedron. As a result, interatomic distances and angles in the tantalum polyhedron show greater variability than those in the aluminum polyhedron.

TABLE 6. SELECTED INTERATOMIC DISTANCES AND ANGLES FOR ALUMOTANTITE

Ta Octahedron			Al Octahedron		
Ta - O(1)a x2	2.06(2)		Al - O(1)a x2	1.88(2)	
- O(1)b x2	2.04(2)		- O(2)b x2	1.87(2)	
- O(2)a x2	1.92(2)		- O(2)f x2	1.94(2)	
< Ta - O >	2.01 Å		< Al - O >	1.89	
O(1)a - O(1)b x2	2.78(2),	85.3(4)	O(1)a - O(1)d x1	2.53(4),	84.6(11)
- O(1)c x2	2.76(2),	84.7(4)	- O(2)b x2	2.75(3),	94.7(8)
- O(1)d x1	2.53(4),	75.7(10)	- O(2)g x2	2.78(2),	89.2(6)
- O(2)a x2	2.88(2),	92.7(7)	- O(2)c x2	2.63(3),	93.7(7)
O(1)b - O(2)a x2	2.88(3),	92.3(7)	O(2)b - O(2)f x2	2.56(4),	84.6(9)
- O(2)d x2	2.94(2),	95.9(8)	- O(2)g x2	2.72(1),	91.4(8)
O(2)d - O(2)a x1	2.92(4),	99.0(11)	O(2)f - O(2)g x1	2.69(4),	88.0(11)
< O - O >	2.83 Å		< O - O >	2.68	
< O-Ta - O >		89.7 °	< O-Ta - O >		90.0

Equivalent Positions

a: *x, y, z* b: 1/2-*x*, 1/2-*y*, 1/2+*z* c: 1/2+*x*, 1/2-*y*, -*z*
d: -*x*, *y*, 1/2-*z* f: 1/2+*x*, 1/2+*y*, 1/2-*z* g: *x*, -*y*, 1/2+*z*

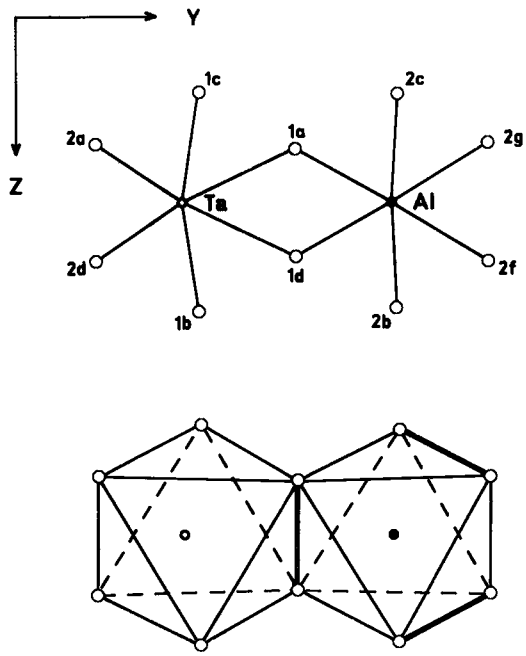

FIG. 3. Coordination polyhedra in alumotantite. Shared edges of polyhedra are shown in thick rule. See Table 6 for the coding of the oxygen atoms.

Simpsonite and Alumotantite Topotaxy

In addition to prismatic crystals of alumotantite, isolated patches of a "cloudy alteration" in Bikita simpsonite can be observed (Macgregor 1946). Gandolfi photographs of this opaque, white material show evidence of both simpsonite and alumotantite. Qualitative microprobe analysis also shows a minor third phase with only Al detectable. These data and paragenetic considerations suggest the phase to be a hydroxide, perhaps gibbsite.

On the basis of the similarity of several of the interplanar spacings of simpsonite to alumotantite, a topotaxic relationship between these minerals is suspected. To investigate this, a fragment of the opaque region was studied by the precession method. The topotaxic relationship was confirmed in the photographs taken, with $X_A \| Z_S$, $Y_A \| [210]_S$, and $Z_A \| [410]_S$, where the subscripts A and S refer to alumotantite and simpsonite, respectively. This alumotantite is twinned; topotaxic control on the twinning has produced threefold rotation twins of alumotantite (about Z_S) in the partially consumed simpsonite. No additional diffraction-maxima indicative of a third phase were observed in the precession photos.

Comparison of the simpsonite structure to that of alumotantite in light of the above relationships shows that the hexagonal closest-packing of oxygen atoms in simpsonite is preserved through the topotaxic reaction that generated the alumotantite (Fig. 4). Hence, the reaction is marked by cation migration through an essentially unchanged array of oxygen atoms.

Optical examination of the Bikita sample shows that both the prismatic alumotantite and the alumotantite in the white patches possess (at least) parallel X axes. By inference, the same crystallographic relationship (less twinning) exists between simpsonite and both alumotantite textural varieties. However, important differences between the two varieties do exist:

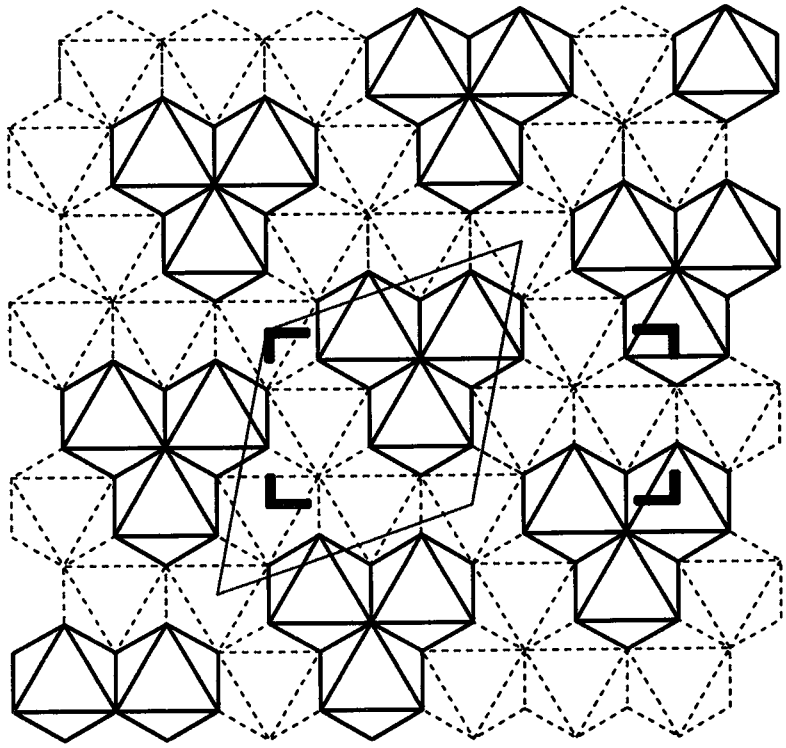

FIG. 4. Projection of the simpsonite structure along Z. Representation of the polyhedra is as in Fig. 1; Ta occupies the octahedra in solid rule, and Al occupies the octahedra in broken rule. The unit cell of simpsonite outlined (fine rule) is two layers deep. The orientation of the alumotantite cell with respect to the hexagonal closest-packing of simpsonite is shown for reference (corners in bold rule).

(1) The prismatic variety occurs as partial replacements of, and overgrowths on, simpsonite, whereas the patchy variety occurs as replacements only.
(2) The prismatic variety occurs along fractures and rims of the simpsonite, whereas the other variety occurs as isolated patches in the interior of simpsonite crystals.
(3) Aluminum silicates (muscovite and albite) rather than aluminum hydroxides occur with the prismatic variety.

Although the two varieties differ greatly in occurrence and paragenesis, the rarity of alumotantite, the similar paragenetic timing of the varieties, and the same topotaxic relationship between simpsonite and both alumotantite varieties suggest a single mechanism of reaction. The observations outlined above suggest the reaction of simpsonite with minor volumes of a late fluid phase with which it was no longer in equilibrium. In particular, an increase in μ_{Ta} is the most feasible cause for the breakdown of simpsonite. A generalized equation describing this reaction is: $Ta^{5+} + 2Al_4Ta_3O_{13}(OH) = 7AlTaO_4 + 2H^+ + Al^{3+}$.

In the interiors of alumotantite crystals, the aluminum released in this reaction is bound up as a hydroxide (*i.e.*, in the white patches). At the rims of, and along fractures in the simpsonite crystal, μSi (and μNa, μK) is sufficiently great to result in the incorporation of the liberated Al^{3+} in aluminum silicates. Quite clearly, the phases formed from the liberated Al^{3+} do not play an active role in simpsonite–alumotantite topotaxy; the same topotaxic relationship between simpsonite and alumotantite is shown by both parageneses despite their differences in mineralogy.

Structural Relations Amongst the $(Al,Ga)(Ta,Nb)O_4$ Oxides

Several aluminum, gallium, tantalum, niobium oxides of ABO_4 stoichiometry have been synthesized; none of these have the alumotantite structure. A review of these compounds and of the conditions of their synthesis reveals important information about the stability of alumotantite.

The rutile-structured polymorphs of the compounds $AlTaO_4$ and $GaTaO_4$ are stable only at very high temperatures (greater than approximately 1500°C: Bayer 1962, Isupova *et al.* 1971). This structure (Fig. 5a) is characterized by completely disordered cations in a hexagonally close-packed array of oxygen atoms. Coordination polyhedra are octahedra and form straight, edge-sharing chains parallel to Z. Chains of one level are linked to those of the next by corner-sharing.

The monoclinic $AlNbO_4$ structure (Fig. 5b) is the most common structure for synthetic ABO_4-type Al, Ga, Ta, Nb oxides. Both fully ordered (*e.g.*, Pedersen 1962) and partly ordered (*e.g.*, Efremov *et al.* 1981) forms have been synthesized. The fully ordered form has edge-sharing dimers of M^{5+}-bearing octahedra; dimers are interconnected along Y by zig-zag chains of M^{3+}-bearing octahedra and along Z by corner-sharing with these chains. The structure is stable up to at least 1700°C for $AlTaO_4$ and up to 1400°C for $AlNbO_4$ and $GaNbO_4$ at atmospheric pressure.

$GaNbO_4$ and $GaTaO_4$ can have the wolframite structure (Fig. 5c). A cation-disordered form of the structure also has been found for $GaTaO_4$ (Bayer 1962). The wolframite structure is the stable modification for $GaTaO_4$ up to at least 1580°C and at atmospheric pressure (Bayer 1962), but is only stable for $GaNbO_4$ above 1.5 kbar (Tamura *et al.* 1980). It is another hexagonal closest-packed structure with octahedrally coordinated cations. All cations of one type occupy a given level parallel to the hexagonal closest packing. Octahedra of any such level are connected by edges to form zig-zag chains parallel to Z and are linked by corner-sharing to chains of adjacent levels.

One other compound has been synthesized for these compositions (Burdese & Borlera 1963), but the structure is unknown. It has no immediate structural similarities with other synthetic ABO_4 compounds or alumotantite in terms of its powder-diffraction properties. Unfortunately, conditions of its stability are poorly known.

From a structural viewpoint, alumotantite (Fig. 5d) is similar to all of these compounds in that it has only octahedrally coordinated cations, and similar to most in that the aluminum polyhedra are present in edge-sharing chains. However, it differs in several important aspects. The total edge-sharing chain in alumotantite is much more intricately branched than in the other structures. Also, the polyhedra that contain the pentavalent cation show a greater degree of polymerization in alumotantite (sheets) than in the other structures (disordered, dimers or chains).

All of the syntheses have been anhydrous, and, except for $GaNbO_4$, performed at atmospheric pressure. The tantalum-bearing compounds do not form below 1000–2000°C under such conditions; similarly, the niobium-bearing ones do not form below 1000°C. In contrast, alumotantite has only been found in late metasomatic assemblages of rare-element-enriched granitic pegmatites. This type of occurrence implies formation in a fluid-rich environment with P(fluid) = P(total) = 1.5 to 3 kbar and with a temperature of formation between 200 and 400°C (*e.g.*, London *et al.* 1983).

In conclusion, we contend that from structural and paragenetic information, alumotantite has never appeared in synthesis studies because these have been conducted under conditions too far

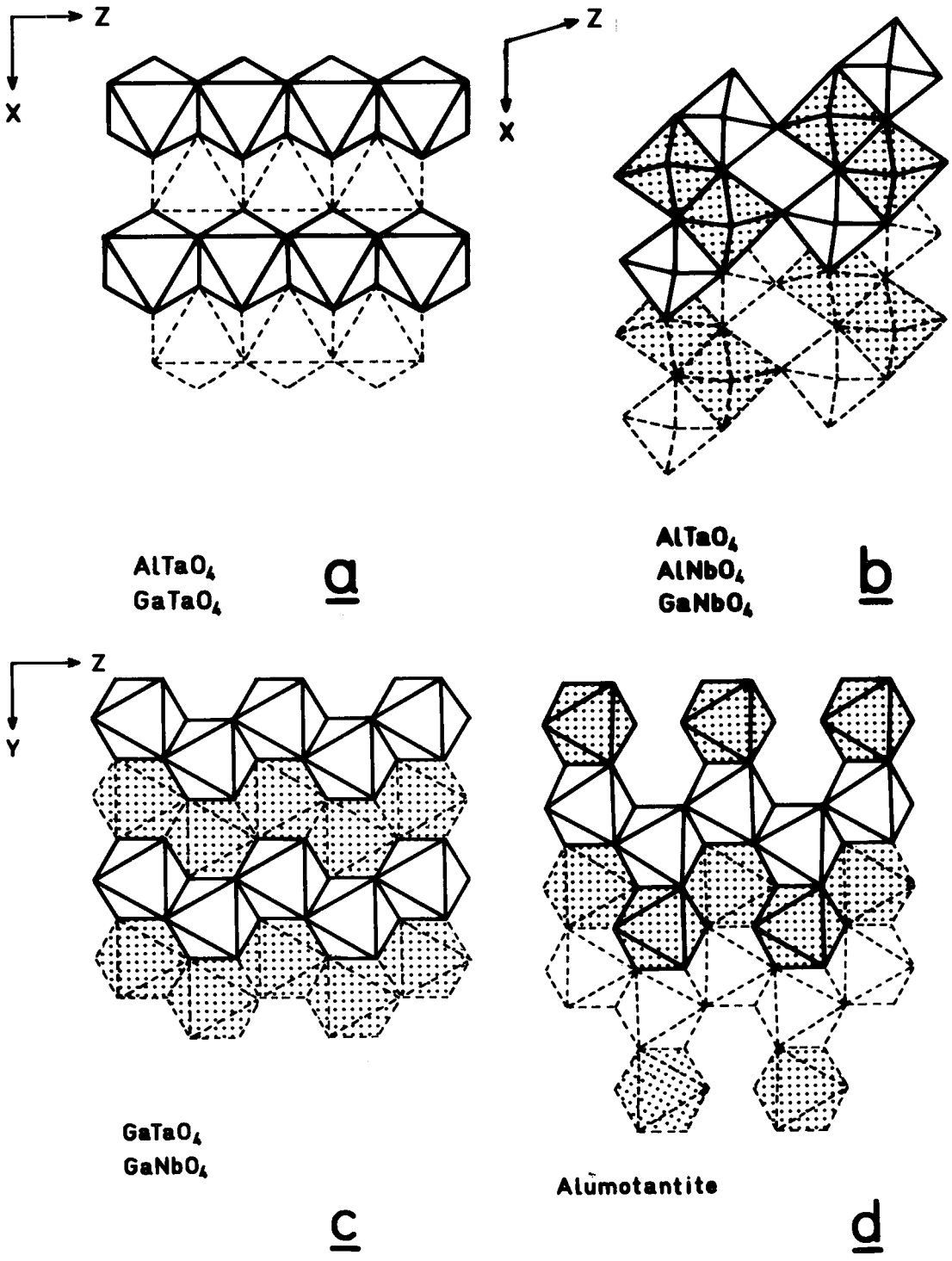

FIG. 5. Projections of ABO_4 structures, where A represents Al and Ga, and B, Ta and Nb. Structure types: (a) rutile, (b) $AlNbO_4$, (c) wolframite, (d) alumotantite. Representation of the polyhedra is as in Fig. 1. For the ordered structures, M^{5+}-bearing polyhedra are stippled, M^{3+}-bearing polyhedra are unshaded.

removed from its stability range. We propose that alumotantite is the stable low-temperature polymorph of $AlTaO_4$.

ACKNOWLEDGEMENTS

We are indebted to J.S. White of the U.S. National Museum of Natural History, Washington, for providing the samples for the study. We thank the Materials Research Institute, McMaster University, for the collection of the X-ray intensity data. Financial support for this work was provided by NSERC grants to FCH and PČ, and NSERC Research Fellowship to FCH and an NSERC Postgraduate Scholarship to TSE.

REFERENCES

BAYER, V.G. (1962): Isomorphic and morphotropic relationships between oxides of the TiO_2-type and related structures. *Ber. Dtsch. Keram. Ges.* **39**, 535-554 (in German).

BROWN, I.D. (1981): The bond-valence method: an empirical approach to chemical structure and bonding. *In* Structure and Bonding in Crystals II (M. O'Keeffe & A. Navrotsky, eds.). Academic Press, New York (1-30).

BURDESE, A. & BORLERA, M.L. (1963): Constanti reticolari e spettrogramma di polveri del niobato di alluminio. *La Ricerca Scientifica, Rend. A* **3**, 1023-1024.

CROMER, D.T. & LIBERMAN, D. (1970): Relativistic calculation of anomalous scattering factors for X rays. *J. Chem. Phys.* **53**, 1891-1898.

_____ & MANN, B.J. (1967): X-ray scattering factors computed from numerical Hartree–Fock wave functions. *Acta Crystallogr.* **A24**, 321-324.

EFREMOV, V.A., TRUNOV, V.K. & EVDOKIMOV, A.A. (1981): Refinement of the structure of aluminum niobate. *Sov. Phys. Crystallogr.* **26**, 172-176.

ERCIT, T.S. (1986): *The Simpsonite Paragenesis. The Crystal Chemistry and Geochemistry of Extreme Ta Fractionation.* Ph.D. thesis, Univ. Manitoba, Winnipeg, Manitoba.

_____, HAWTHORNE, F.C. & ČERNÝ, P. (1986): The crystal structure of bobfergusonite. *Can. Mineral.* **24**, 605-614.

FINGER, L.W. (1969): RFINE. A Fortran IV computer program for structure factor calculation and least-squares refinement of crystal structures. *Geophys. Lab., Carnegie Inst. Wash.* (unpubl.).

ISUPOVA, E.N., GODINA, N.A. & KELER, E.K. (1971): Reactions in the systems Al_2O_3–Nb_2O_5 and Al_2O_3–Ta_2O_5. *Izv. Akad. Nauk SSSR, Neorg. Mater.* **6**, 1465-1469 (in Russ.).

LONDON, D.L., SPOONER, E.T.C. & ROEDDER, E. (1983): Fluid-solid inclusions in spodumene from the Tanco pegmatite, Bernic Lake, Manitoba. *Carnegie Inst. Wash. Yearb.* **82**, 334-339.

LOVE, G. & SCOTT, V.D. (1978): Evaluation of a new correction procedure for quantitative electron probe microanalysis. *J. Phys.* **D11**, 1369-1376.

MACGREGOR, A.M. (1946): Simpsonite and other tantalates from Bikita, southern Rhodesia. *Mineral. Mag.* **27**, 157-165.

MANDARINO, J.A. (1976): The Gladstone–Dale relationship. I. Derivation of new constants. *Can. Mineral.* **14**, 498-502.

PEDERSEN, B.G. (1962): The crystal structure of aluminum niobium oxide ($AlNbO_4$). *Acta Chem. Scand.* **16**, 421-430.

POUGH, F.H. (1945): Simpsonite and the northern Brazilian pegmatite region. *Geol. Soc. Am. Bull.* **56**, 505-514.

REED, S.J.B. (1965): Characteristic fluorescence corrections in electron-probe microanalysis. *Brit. J. Appl. Phys.* **16**, 913-926.

RUCKLIDGE, J. & GASPARRINI, E. (1969): Specifications of a computer program for processing electron micro-probe analytical data (EMPADR VII). *Dep. Geol., Univ. Toronto, Toronto, Ontario.*

SHANNON, R.D. (1976): Revised effective ionic radii and systematic studies of interatomic distances in halides and chalcogenides. *Acta Crystallogr.* **A32**, 751-767.

TAMURA, S., WAKAKUWA, M. & HIROTA, K. (1980): Polymorphic transition of $GaNbO_4$ under high pressures. *J. Mater. Sci.* **15**, 2128-2129.

VOLOSHIN, A.V., MEN'SHIKOV, YU.P. & PAKHOMOVSKII, YA.A. (1981): Alumotantite and natrotantite, new tantalum minerals. *Zap. Vses. Mineral. Obshchest.* **110**, 338-345 (in Russ.).

WILES, D.B. & YOUNG, R.A. (1981): A new computer program for Rietveld analysis of X-ray powder diffraction patterns. *J. Appl. Crystallogr.* **14**, 149-151.

Received November 3, 1983, revised manuscript accepted February 12, 1992.